PROGRESS IN PHOTOVOLTAICS: RESEARCH AND APPLICATIONS
Prog. Photovolt: Res. Appl. 2000; **8**: 591–602

Research

Influence of Surface Composition on Back-contact Performance in CdTe/CdS PV Devices†

Dean Levi*, David Albin and David King
National Renewable Energy Laboratory, 1617 Cole Boulevard, Golden, CO 80401, USA

The atomic composition of the surface of the CdTe layer in a CdTe/CdS photovoltaic (PV) device has a significant influence on the quality of the electrical contact to this layer. This paper reports the results of a systematic study that correlates the composition of the back surface as measured with X-ray photoelectron spectroscopy (XPS) with pre-contact processing and device performance. We found that certain processing steps produce an oxide layer that degrades device performance by producing a metal–oxide–semiconductor (MOS) contact, rather than the intended metal–semiconductor, Schottky barrier contact. We also found that the as-deposited CdTe film is cadmium-rich for several hundred angstroms at the back surface. This* n*-type layer may impede current flow for majority holes, degrading device performance. Published in 2000 by John Wiley & Sons, Ltd.

INTRODUCTION

An essential issue in commercialization of CdTe-based thin-film solar cells is developing a method for making a stable, low-resistance back contact.[1] Because no metal has a work function larger than the work function of *p*-type CdTe, a fundamental problem exists in forming low-resistance contacts. The normal alternative of producing low-resistance tunneling contacts by high doping of the CdTe surface is difficult because of the complexities in doping CdTe to high hole densities. Both Ponpon[2] and Fahrenbruch[3] have reviewed these issues in previous papers.

Numerous deposition methods exist for producing high-efficiency CdTe/CdS PV devices.[1] All of these methods require several post-deposition processing steps.[4–6] An important step used in all of these processes is exposure to $CdCl_2$ in conjunction with annealing. As originally developed, the $CdCl_2$ treatment required mixing $CdCl_2$ powder into the Cd/Te mixture prior to film deposition.[7] The process was subsequently refined into a post-deposition dip in a $CdCl_2$ solution followed by annealing.[8] As the technology has progressed, several research groups have developed a vapor-based $CdCl_2$ treatment to replace the solution-based process.[9–11] A primary goal in CdTe PV technology is to develop an all-dry fabrication process. Such a process is amenable to continuous, in-line production, which is a promising

* Correspondence to: Dean Levi, NREL, 1617 Cole Boulevard, Golden, CO 80401, USA.
E-mail: Dean_Levi@NREL.gov.

Contact/grant sponsor: US Department of Energy; contract/grant number: DE-AC36-99GO10337.

Received 29 January 2000
Revised 10 May 2000

route for low-cost, high-volume manufacturing of CdTe/CdS photovoltaics. This study examines the relationships between the NREL post-deposition processes, atomic composition near the CdTe back surface, and device performance.

EXPERIMENTAL DETAILS

Thin-film deposition

The polycrystalline CdTe/CdS thin films used in this study were deposited using close-spaced sublimation (CSS) at the National Renewable Energy Laboratory (NREL). Samples used for surface characterization and device fabrication consisted of multi-layer CdTe/CdS/SnO_2/7059-glass structures representative of typical NREL CdTe/CdS devices.[8] The SnO_2 layer was deposited using tetramethyltin chemical vapor deposition (CVD) and was a bilayer structure comprised of both a high- and low-resistance layer.[12] The 800-Å-thick CdS layer was deposited by chemical bath deposition (CBD). The 8-μm-thick CdTe films were deposited by close-spaced sublimation (CSS) at a substrate temperature of 620°C. Deposition was at a rate of ~2 μm/min in an ambient of 1 torr oxygen/15 torr helium. The CdS layer was processed using a thermal etch prior to CdTe deposition.[12] Structures were allowed to cool in the He:O_2 ambient. Post-deposition processing is described in the next section.

$CdCl_2$ and back-contact processing

The NREL CdTe research program is currently in transition from use of a solution-based, wet $CdCl_2$ treatment, to a vapor-based, dry $CdCl_2$ treatment. In this study we compare and contrast the surface conditions associated with sequential processing steps for each $CdCl_2$ process type.

For the wet $CdCl_2$ treatment, the samples are placed in a boiling, 50%-saturated $CdCl_2$–methanol solution for 15–20 min. The samples are removed from the solution and blown with dry nitrogen to distribute the $CdCl_2$ uniformly over the surface. These samples are then annealed at 400°C for 30 min in a flowing atmosphere of 25 sccm O_2 and 100 sccm He. Following the annealing step, the samples are etched in a 350 : 4 :140 mixture of HNO_3 : H_3PO_4 : H_2O (NP etch).[14] The etch process is continued until bubbles cover the surface—an indication that the surface has been converted to elemental tellurium.[15] The samples are rinsed in running deionized (DI) water to stop the etch process. Following the rinse, a mixture of Cu-doped HgTe in Electrodag 114 is applied, and the sample is annealed for 30 min at 260°C. Finally, silver paint is applied, and the device is annealed at 100°C in air.[6]

In the NREL, vapor-$CdCl_2$ treatment, the samples are exposed to $CdCl_2$ vapor at 400°C in a modified CSS chamber in the laboratory ambient atmosphere.[11] Both the $CdCl_2$ source and the substrate are held at 400°C for 5 min. After this step, the samples are rinsed in flowing DI water, then etched in NP etch. The remainder of the contact application procedure is the same as above. NREL researchers regularly achieve devices with efficiencies over 13% using either vapor or the solution $CdCl_2$ treatments.

Processing conditions

To gain a clearer understanding of the effects of the post-deposition processing, X-ray photoelectron spectroscopy (XPS) was used to characterize the back-surface composition after each post-growth processing step. PV devices were also fabricated at each step of processing to correlate back-surface

Table I. Processing conditions for samples investigated for back-surface composition and device performance. SCC stands for solution-$CdCl_2$ treatment, while VCC stands for vapor-$CdCl_2$ treatment

SCC only	SCC anneal	SCC/anneal/DI	SCC/anneal/ vacuum anneal	SCC/anneal/ nitric acid/DI	SCC/anneal/ DI/NP/DI
	VCC	VCC/DI	VCC/vacuum anneal	VCC/DI/nitric acid/DI	VCC/DI/NP/DI

composition with device performance. Table I delineates the back-surface processing conditions investigated in this study. SCC stands for solution-$CdCl_2$ treatment, while VCC stands for vapor-$CdCl_2$ treatment. The sample labeled SCC-only underwent the $CdCl_2$-dip, but no anneal. There is no corresponding processing step in the vapor-$CdCl_2$ process because annealing and $CdCl_2$ exposure occur simultaneously in the vapor treatment.

In addition to the standard conditions described above, two exploratory processing steps have been included in the matrix of samples. Waters *et al.*[16] investigated the cleansing effects of annealing under vacuum, and of a weak nitric acid solution. These conditions have been included as intermediary between a simple DI rinse, and the extensive etching produced by the NP etch. The vacuum annealing was performed in a modified CSS chamber. Pressure was about 10^{-3} torr, temperature was 400°C, and the sample was in proximity to a clean surface of borosilicate glass. Anneal time was 10 min, and the sample temperature was maintained 5°C above the borosilicate glass. The nitric acid etch consisted of 3 ml of 15·9 M nitric acid in 100 ml of H_2O. Etch time was 60 s, followed by a DI rinse to halt the etching process.

Separate samples were prepared for XPS characterization and for device fabrication. XPS samples were either measured immediately after processing, or stored in dry nitrogen between processing and characterization. Samples for device fabrication were stored in a dry box in laboratory ambient until processed into devices and characterized.

XPS characterization

XPS analyses were carried out with a Physical Electronics 5600 photoelectron spectrometer operating at a typical base pressure of 2×10^{-10} torr. Photoelectrons were excited with monochromatic A1 K α_X-radiation, with an anode power of 300 W at 15 kV. Photoelectrons were collected at 45° from the sample normal and resolved with a hemispherical analyzer at a pass energy of 58·7 eV. Depth profiles were accomplished with a Perkin-Elmer model 04-303A differentially pumped ion gun using a 1-kV Ar^+ ion beam rastered over a 3×3-mm area. The X-ray exposed- and analyzer acceptance-area is approximately 1 mm^2, centered in the raster region. This eliminates artifacts due to redeposition of sputtered material. Sputter depth profiles were performed to maximize the depth resolution; hence, XPS data were collected with a sputtering interval of 20 s. Areas of the resulting photoelectron peaks were used to determine atomic concentrations after each sputter interval, and thus, generate the compositional depth profiles. XPS is sensitive to approximately 0·1 at % composition. Elements present at concentrations lower than this limit are not detectable using XPS.

Sputter rate calibrations were performed on several CSS CdTe films by sputtering a 0·1–0·2 micron deep crater and measuring its dimensions with a stylus profilometer. The ion beam parameters used result in an average sputter rate of 17 Å per minute. This erosion rate corresponds to the removal of about 5.7 Å, or slightly less than two monolayers of material between each XPS analysis. This slow sputter rate, combined with short intervals between XPS analyses, enables an accurate determination of composition as a function of depth in the near-surface region of these films. It should be noted that the RMS roughness of approximately 1 μm on the surface of these films does not interfere with the depth resolution of the XPS depth profiles. This is because the height variation occurs on a relatively large horizontal scale of approximately 5 μm, and because the sputtering process removes only 0·06%

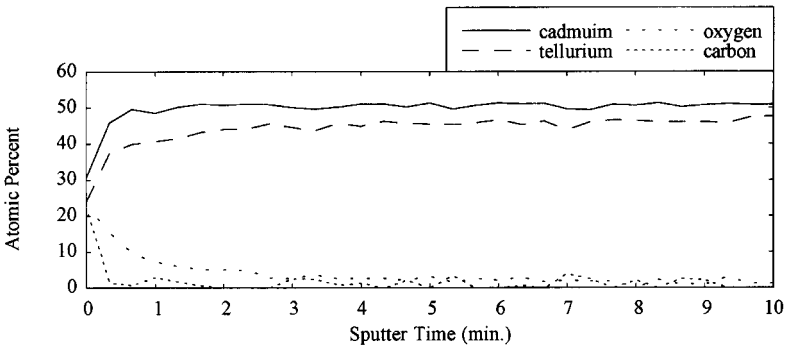

Figure 1. XPS depth profile of as-deposited sample

of the 1 μm height variation between each XPS survey. We have verified that compositional changes occurring in less than 1 min of sputtering time are repeatable, and therefore valid data.

RESULTS

Surface composition

The atomic composition within 10 min sputter time (170 Å) of the surface of each sample was characterized by XPS depth profiling. The atomic percentages of the elements tellurium, cadmium, oxygen, chlorine, sulfur, and carbon were measured. No other elements were present at levels detectable by XPS.

Figure 1 presents the composition profile for the as-deposited sample prior to any treatment. There was no detectable chlorine on this sample. Carbon is present for the first half-minute of sputtering, or approximately 8 Å, most likely due to hydrocarbons adsorbed on the surface. Interestingly, the sample contains 20% oxygen at the surface, which drops below the detection limit in 8–10 min (140–170 Å) of sputtering. There is also an excess of cadmium relative to tellurium. Near the surface, these values are about 50% and 40%. These percentages gradually close to roughly 51% and 47% at 10 min (170 Å). We profiled the composition to a depth of 3000 Å and found that the composition is 50·5% cadmium and 49·5% tellurium at that depth.

It is not clear at this time if the material in the bulk is actually non-stoichiometric, or if the 1·02 : 1·0 cadmium to tellurium ratio is due to a difference between the sensitivity factors defined for the XPS instrument and the actual instrumental sensitivities to cadmium and tellurium in polycrystalline CdTe. We have attempted to calibrate our measurements using comparative measurements of single crystal and polycrystalline CdTe using XPS, Auger Electron Spectroscopy, Rutherford backscattering, Electrode Probe Micro-Analysis, and Inductively Coupled Plasma analysis. Initial results are generally in agreement with our XPS results, yet there is some confusion, as the single crystal samples are farther from stoichiometric than the polycrystalline samples. We are currently performing a comparative study to determine the correct sensitivity factors and will report those results in a later paper.

For the purposes of this study, it is clear that the material near the surface is cadmium-rich compared to the bulk. This has important implications for contact formation, as it is known that cadmium interstitials and tellurium vacancies both form shallow donors which could make the near-surface region *n*-type.[17] Such an *n*-type region would impede the flow of majority-carrier holes through the metallic contact at the back surface, producing a relatively high-resistance back contact and limiting the efficiency of the solar cell.

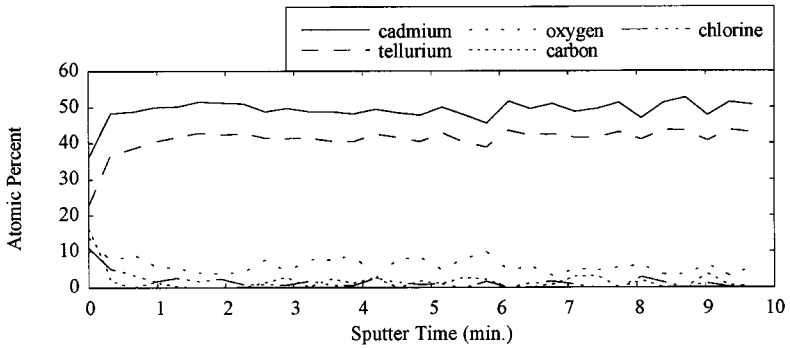

Figure 2. XPS depth profile after the vapor $CdCl_2$ treatment

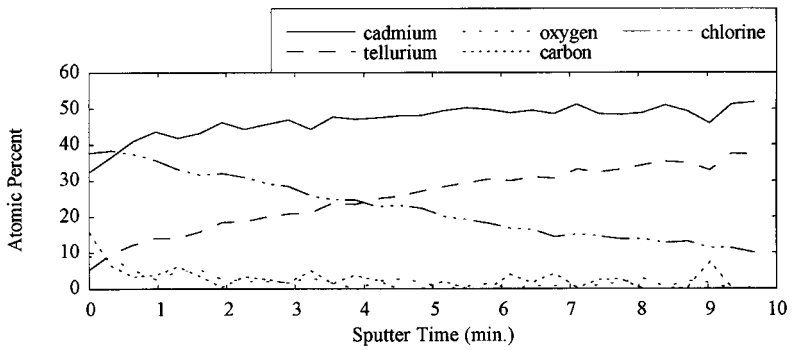

Figure 3. XPS depth profile after the $CdCl_2$-methanol dip

Figure 2 shows the XPS depth profile for the VCC-only sample. This sample is quite similar in composition to the as-deposited sample. The cadmium excess is slightly higher, with roughly 50% cadmium to 38% tellurium near the surface. The oxygen content at the surface has been reduced to 10%, but this composition persists deeper into the sample, measuring 4% after 10 min of sputtering. This result is not surprising, as the VCC process involves annealing in a helium-oxygen gas mixture. There is also chlorine present at a concentration of 10% at the surface, falling to 1–2% after 3 min of sputtering. We conclude that $CdCl_2$ has been incorporated into the near-surface region of the sample.

Figure 3 shows the depth profile following the $CdCl_2$-methanol dip, but prior to the 400°C air anneal. The surface is composed primarily of cadmium and chlorine, with relatively small amounts of tellurium, oxygen, and carbon. The chlorine signal decreases steadily from the surface, while the tellurium signal increases proportionally. It appears that this surface is composed of a mixture of $CdCl_2$ and CdTe, possibly with some component of chemical compounds produced by interaction between $CdCl_2$ and CdTe. Following the dip in the $CdCl_2$ solution, the sample is annealed in laboratory ambient air at 400°C for 30 min.

The results of the annealing step are shown by the profile in Figure 4. The surface composition is radically different from the SCC-only sample. The oxygen content near the surface is quite high at approximately 50%, and remains relatively high at 25% after 10 min of sputtering. Chlorine content has been reduced, yet it is relatively high in comparison with the VCC sample. There is a thin layer of carbon at the surface, as in the VCC and as-deposited samples. The Cd : Te ratio is nearly 3 : 1 at the surface and falls to about 1·5 : 1 after 10 min sputter time. These results indicate a surface that is primarily composed of oxides, and contains 2–6 at % $CdCl_2$.

The surface compositions illustrated by the profiles in Figures 2 and 4 comprise the surface conditions prior to the pre-contact cleaning steps. As discussed in the previous section, we have investigated the

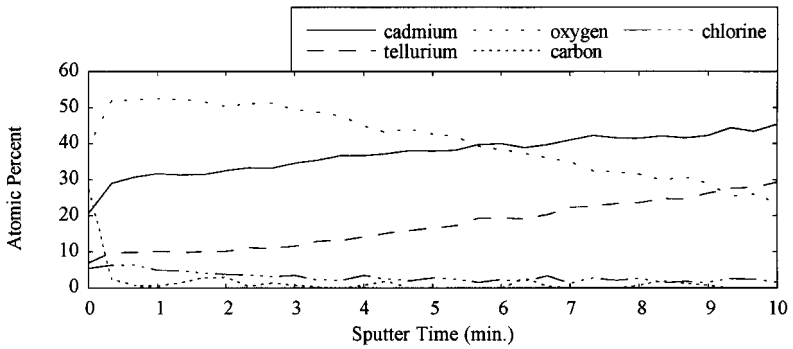

Figure 4. XPS depth profile after air-annealing of the solution $CdCl_2$ sample

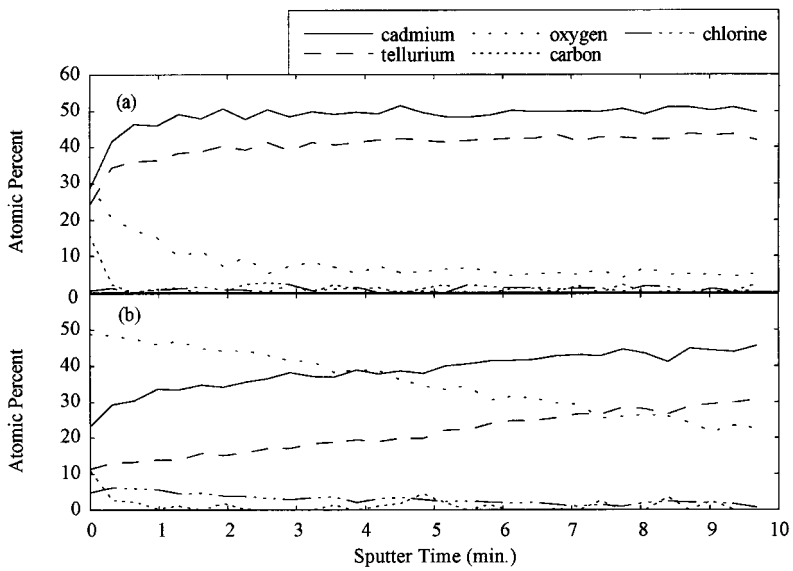

Figure 5. XPS depth profiles following a 30 s rinse in flowing deionized water for (a) the vapor-$CdCl_2$ sample and (b) the solution-$CdCl_2$-annealed sample

effects of four different cleaning steps. The simplest cleaning procedure involves rinsing the sample surface in running DI water for about 30 s. The effects of this procedure on the vapor-$CdCl_2$ and solution/annealed-$CdCl_2$ samples are shown in Figures 5(a, b).

The profile for the VCC/DI sample shows that the oxygen content has doubled from 15% to 30% at the surface, but drops back to its previous levels after 3–4 min of sputtering. The VCC-only sample had nearly 10% chlorine at the surface, while the VCC/DI sample has less than 1%. Both samples have very low amounts of chlorine at depths greater than 1 min of sputtering. Thus, the DI rinse removes chlorine from the surface, but oxidizes the near-surface region of the VCC sample. In contrast, the SCC/anneal sample is almost unchanged by the DI rinse. There is a reduction of adsorbed hydrocarbons at the surface, and a slight reduction in the oxygen content. It appears that the DI rinse has little effect on the SCC/anneal sample.

The next pre-contact cleaning procedure investigated was vacuum annealing. The XPS profiles for the VCC/vacuum anneal and SCC/anneal/vacuum anneal samples are shown in Figure 6 (a and b, respectively). For the solution-$CdCl_2$ sample, the effects of vacuum annealing are virtually identical to those produced by the DI rinse. The only observed difference is the vacuum annealed sample has slightly

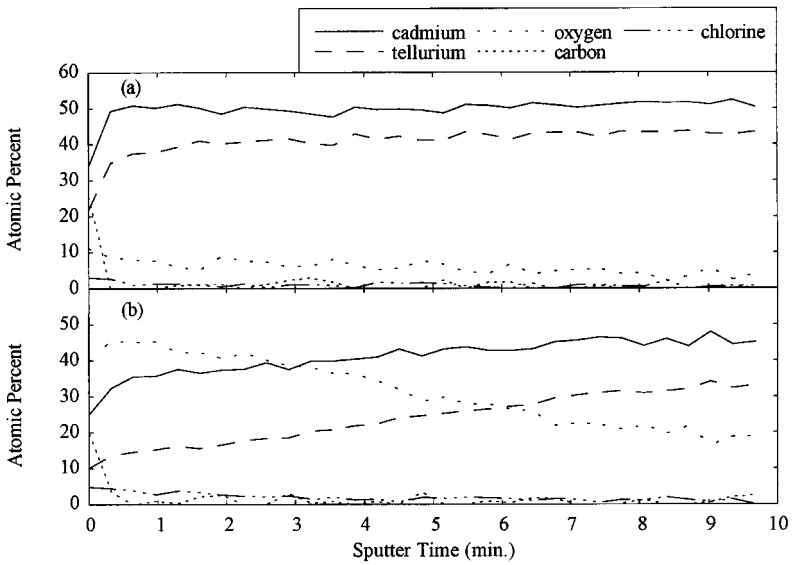

Figure 6. XPS profiles after vacuum annealing at 400°C for 30 min for (a) the vapor-$CdCl_2$ sample and (b) the solution-$CdCl_2$-annealed sample

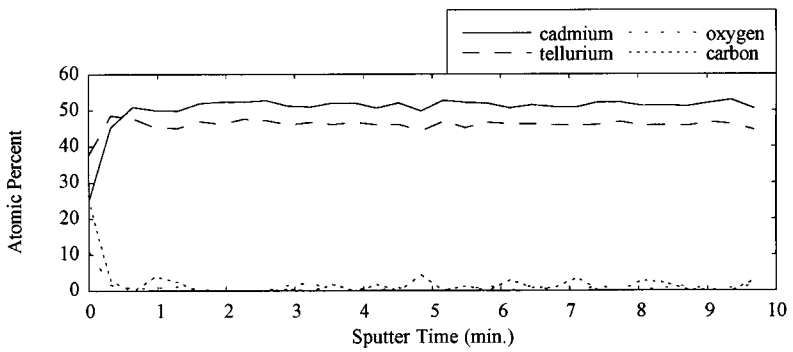

Figure 7. XPS profile of annealed solution-$CdCl_2$ sample after nitric acid etch and DI rinse

more carbon at the surface. For the vapor-$CdCl_2$ sample, there are subtle differences between the DI rinse and the vacuum annealing. The vacuum annealing step slightly reduces the oxygen content instead of increasing it. Also, vacuum annealing is slightly less effective in removing chlorine.

The second experimental pre-contact cleaning procedure was etching in dilute nitric acid (HNO_3) for 60 s followed by a brief DI rinse. In this case, the XPS profiles of the solution-$CdCl_2$ and vapor-$CdCl_2$ samples are identical. The profile for the SCC/anneal/HNO_3/DI sample is shown in Figure 7. This surface is significantly cleaner than any of the preceding profiles. Approximately the first monolayer is tellurium-rich. The rest of the profile shows Cd and Te percentages of about 50% and 47%, respectively. This is very close to the percentages found in the as-deposited sample. As discussed above, uncertainty in sensitivity factors makes it difficult to pin down exact stoichiometry, but this sample clearly has a lower Cd : Te ratio than any of the previous $CdCl_2$-treated samples.

The standard pre-contact cleaning step used in NREL CdTe/CdS device processing is etching in a 350 : 4 : 140 mixture of $HNO_3 : H_3PO_4 : H_2O$ (NP etch). The sample is etched until bubbles cover the surface, indicating that the surface has been converted to elemental tellurium. Rinsing in running DI water is used to halt the etching process. As with the nitric acid etch shown above, after the NP etch,

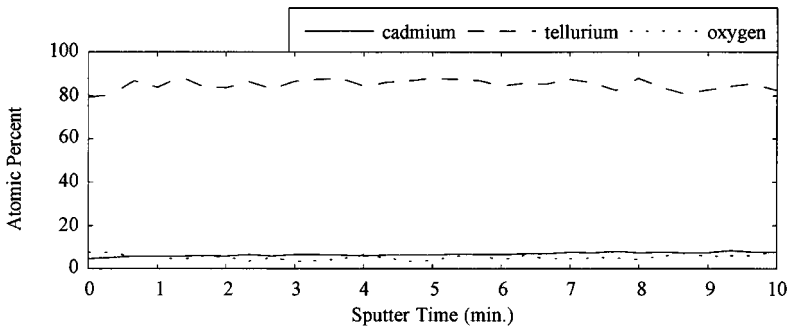

Figure 8. XPS profile of the vapor-$CdCl_2$ sample after NP etching and rinsing in DI water

both vapor-$CdCl_2$ and solution-$CdCl_2$ samples have virtually identical XPS profiles. The profile for the VCC/NP/DI sample is shown in Figure 8. As established in previous studies,[15] we find that the surface is primarily tellurium, with small amounts of cadmium and oxygen. We conclude that the NP-etched surface is composed of slightly oxidized elemental tellurium with small amounts of cadmium, possibly as CdTe.

Table II presents a summary of the atomic percentages of oxygen and chlorine for the samples in this study. The depth profiles have been parameterized in terms of atomic percent (at % after 10 min of sputtering, or the sputter time at which the at % falls below the XPS detection limit.

Device characterization

To correlate the back-surface composition with the quality of the back contact, we have fabricated devices from samples at each step of the processing, as measured using XPS. Considerable care has been taken to ensure that all of the devices are identical except for their back-surface processing. For each processing condition, two devices were fabricated and their light and dark current–voltage (J–V) curves were measured. The values of open-circuit voltage, V_{OC}, and short-circuit current density, J_{SC}, are very consistent for all samples that underwent a $CdCl_2$ treatment. This consistency demonstrates that the bulk properties of all of the films are very similar, as V_{OC} depends primarily on the quality of

Table II. XPS-measured at % for oxygen and chlorine at the surface and after 10 min sputtering (~170 Å depth). Depth profiles are approximately linear with depth, except for oxygen in the VCC/DI sample

Sample processing	At % oxygen at surface	At % oxygen at 10 min, or sputter time at% < XPS limit	At % chlorine at surface	At% chlorine at 10 min, or sputter time at% < XPS limit
As deposited	20	3 min	<XPS limit	<XPS limit
SCC only	15	2 min	40	10
SCC/anneal	50	25	10	2
SCC/anneal/DI	49	20	5	1
SCC/anneal/vacuum anneal	45	20	5	1
SCC/anneal/DI/HNO_3	10	0·5 min	trace	<XPS limit
SCC/anneal/DI/NP etch	6	6	trace	trace
VCC only	10	2	10	<XPS limit
VCC/vacuum anneal	9	5	2	<XPS limit
VCC/DI	30	5 at 4 min 5 at 10 min	1	1
VCC/DI/HNO_3	8	0·3 min	<XPS limit	<XPS limit
VCC/DI/NP etch	6	6	trace	trace

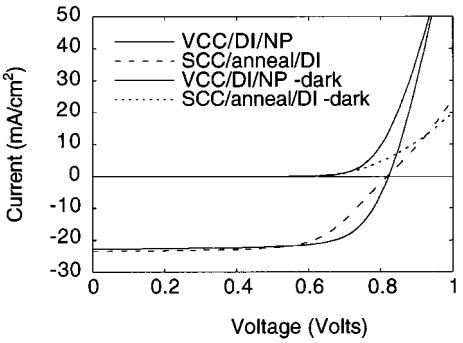

Figure 9. $J-V$ curves for devices fabricated from the VCC/DI/NP and SCC/anneal/DI samples. Both light and dark $J-V$ curves are shown. Solid lines are for the VCC/DI/NP sample, dashed lines are for the SCC/anneal/DI sample

the CdTe–CdS junction, and J_{SC} is primarily a function of optical absorption and carrier collection efficiency. The device parameters that are sensitive to changes in back surface quality are the fill factor (FF), and the series resistance (R_s).

Light and dark $J-V$ curves for devices characteristic of the higher- and lower-efficiency samples in this study are shown in Figure 9. The solid lines are for the VCC/DI/NP sample, and the dashed lines are for the SCC/anneal/DI sample. It is clear that both devices have almost identical V_{OC} and J_{SC}. The primary difference between the two $J-V$ curves is in the slope of the curve for voltages greater than 0·7 V. This slope is a function of the R_S, which can in turn be related to the contact resistance.

The primary measure of the quality of the back contact is the contact resistance, R_C. It is not practical to directly measure R_C in these devices, because standard techniques such as the transfer length method are dominated by the high in-plane resistivity of polycrystalline CdTe. Typical values of in-plane, dark resistivity are in excess of 1 G Ω-cm, while in-plane resistivity in the light is on the order of 40 M Ω-cm. It is possible to determine the total series resistance of the device, R_S, using a method described below. In forward bias, near V_{OC}, the series resistance, R_S, can be expressed as the sum of the back-contact resistance plus the lumped resistance of the rest of the device, R_O

$$R_S = R_O + R_C \tag{1}$$

Because the devices in this study are identical except for their back-surface treatments, we propose that changes in R_S are primarily due to changes in R_C.

Series resistance can be calculated from the $J-V$ curve using an analytical technique established by Sites[18] for the $J-V$ analysis of polycrystalline solar cells. Using the standard photodiode equation and assuming high shunt resistance (which is the case for the devices in this study), one can derive an equation of the form

$$\left(\frac{dV}{dJ}\right) = R_S + \frac{AkT}{q}(J + J_{SC})^{-1} \tag{2}$$

where q is the electronic charge, A is the diode quality factor, k is the Boltzmann's constant, and T is the temperature. In the dark, the inverse current term is reduced to J^{-1}. The series resistance is determined by taking the intercept of (dV/dJ) vs J^{-1}. We have used this formalism to calculate values of R_S for each of the devices studied.

The $J-V$ parameters for the devices in this study are presented in Table III. For each processing condition, these values are averages over two devices. The values of R_S presented in the table are calculated from the dark $J-V$ curves measured at 25°C. The as-deposited sample has significantly lower values of efficiency, V_{OC} and J_{SC} compared to the rest of the devices because it lacks a $CdCl_2$ treatment. With that exception noted, the values of V_{OC} range from 804 mV to 820 mV, and the values of J_{SC} range from 22·7 mA/cm^2 to 23·8 mA/cm^2. The small scatter in these parameters demonstrates the consistency

Table III. Device parameters for various back-surface treatments. Each parameter is an average over two devices

Sample processing	R_S (Ω-cm^2)	Efficiency (%)	FF	V_{OC} (mV)	J_{SC} (mA/cm^2)
As deposited	7·0	8·7	55·0	719	22·0
SCC only*	NA	NA	NA	NA	NA
SCC/anneal	6·9	12·05	63·3	812	23·5
SCC/anneal/DI	8·0	12·35	65·5	815	23·4
SCC/anneal/vacuum anneal	6·8	11·9	61·8	808	23·8
SCC/anneal/DI/HNO_3	5·3	12·85	66·3	818	23·7
SCC/anneal/DI/NP etch	1·3	13·05	69·7	804	23·2
VCC only	2·5	13·1	68·0	820	23·6
VCC/vacuum anneal	3·2	13·1	67·1	818	23·8
VCC/DI	3·7	12·25	63·5	818	23·5
VCC/DI/HNO_3	2·9	12·5	65·2	816	23·4
VCC/DI/NP etch	1·7	13·3	71·2	816	22·7

* No device was measured for the SCC-only sample because it was not practical to fabricate a device due to the thick $CdCl_2$ residue present on the back surface.

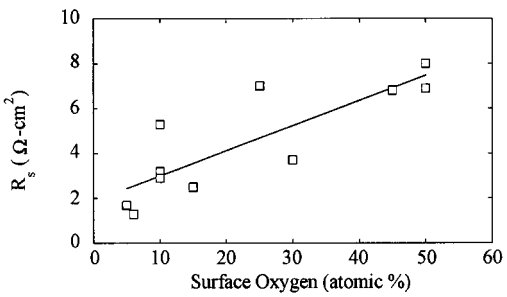

Figure 10. Devices series resistance vs surface oxygen content

of the junction and bulk properties of the films used to fabricate these devices. In contrast, R_S varies from 1·3 Ω-cm^2 to 8·0 Ω-cm^2. As we have established above, this large variation in series resistance should primarily be due to differences in contact resistance. The variations in R_S correlate well with the properties of the back surface as measured by XPS.

The two NP-etched samples have R_S-values of 1·3 and 1·7 Ω-cm^2. XPS measurements on these samples show that their surfaces are primarily elemental tellurium. It is known that elemental tellurium is a degenerate, narrow-gap, *p*-type semiconductor[19] that provides a good contact to *p*-type CdTe. This is consistent with the result that the two NP-etched samples have the lowest R_S, which implies the lowest contact resistance.

Figure 10 shows how R_S depends on the oxygen content at the surface. The line in the figure is a linear fit to the data points. It is clear that R_S, and hence R_C, is an approximately linear function of the oxygen content at the surface of the CdTe absorber layer. This is consistent with formation of an MOS back contact for the devices with significant amounts of oxygen, and a metal-semiconductor Schottky barrier contact for those devices with very little oxygen. Ongoing experiments will study the nature of these contacts through barrier height measurements, etc. Such studies should provide a clearer explanation of the nature of the back contact in these devices.

Discussion

Different steps in the post-deposition processing produce varying degrees of oxidation and contamination of the CdTe surface. The surface of the as-deposited sample is moderately oxidized, and

produces a back contact of moderate resistance. The vapor-$CdCl_2$ process is quite clean, leaving relatively little $CdCl_2$ residue and actually reducing the amount of oxygen present on the surface. Deposition of the contact directly after vapor-$CdCl_2$ treatment results in a low-resistance contact. In contrast, the solution $CdCl_2$ process is relatively dirty, leaving large amounts of $CdCl_2$ residue after the $CdCl_2$ dip. Air-annealing of this surface significantly reduces the amount of $CdCl_2$ residue, but greatly increases the degree of oxidation. The SCC/annealed surface produces a relatively poor, high-resistance contact.

Rinsing in DI water left the SCC/annealed surface essentially unchanged, and produced a contact of equally high resistance. Rinsing in DI water increased the oxidation of the VCC surface, and resulted in a correspondingly higher resistance contact. Vacuum annealing did not change the surface composition or the contact resistance for the VCC sample. Vacuum annealing appeared not to change the SCC/annealed surface, yet the resistance decreased somewhat. We do not presently have a clear explanation for this result.

Etching with the NREL standard NP etch produced surfaces that were primarily elemental tellurium for both the VCC and SCC/annealed samples. As we would expect from previous studies, these surfaces produced very low resistance contacts. Etching with dilute nitric acid produced very clean surfaces for both the VCC and SCC/annealed samples. These surfaces were tellurium-rich for the first one or two monolayers. After that they had the same stoichiometry as measured in the as-deposited sample. Both of these samples produced very low resistance contacts. This result is somewhat surprising, as it is generally believed that a layer of tellurium is needed to produce the proper band line-up between the *p*-type CdTe and a metallic contact. It is possible that the copper-doped HgTe that is applied in the contact application step is providing an adequate band line-up, or it is also possible that the copper in the HgTe is doping the near-surface region of the CdTe enough to produce a narrow Schottky barrier. More research needs to be done to clarify this point.

CONCLUSIONS

Characterization of the back-surface composition using XPS has shown that different steps in the post-growth processing of CdTe/CdS devices at NREL produce varying degrees of oxidation and contamination. The surface properties correlate very well with the contact resistance deduced from measurements of device series resistance. The surface of the as-deposited samples is not clean enough to produce a good contact, but vapor-$CdCl_2$ treatment appears to provide the cleaning necessary to produce a low-resistance contact. It is clear that a great deal of care needs to be taken to ensure that the surface of the CdTe is not inadvertently contaminated during post-deposition processing. With proper processing and handling it should be possible to eliminate chemical etching steps from the pre-contact processing without reducing the quality of the back contact.

Acknowledgements

We wish to thank Yoxa Mahathongdy for assistance with vapor $CdCl_2$ treatments and device fabrication, Rosine Ribeline for chemical bath deposition of the CdS layers; and Pete Sheldon, Tim Gessert, and Brian Keyes for their careful reading of the manuscript. This work was supported by the US Department of Energy under Contract No. DE-AC36-99GO10337.

REFERENCES

1. Birkmire RW, Meyers PV. Processing issues for thin-film CdTe cells and modules. In *Proceedings of the First World Conference on Photovoltaic Energy Conversion*, Waikaloa, Hawaii, 1994. IEEE, 1995; 76–82.

2. Ponpon JP. A review of ohmic and rectifying contacts to cadmium telluride. *Solid State Electronics* 1985; **28**: 689–706.
3. Fahrenbruch AL. Ohmic and rectifying contacts and doping of CdTe. 1987, *Solar Cells* **21**: 399–412.
4. Ferekides CS, Dugan K, Ceekala V, Killian J, Oman D, Swaminathan R, Morel DL. Effects of CdS processing and glass substrates on the performance of CdTe solar cells. In *Proceedings of the First World Conference on Photovoltaic Energy Conversion*, Waikaloa, Hawaii, 1994. IEEE, 1995; 99–102.
5. McCandless BE, Qu Y, Birkmire RW. A treatment to allow contacting CdTe with different conductors. In *Proceedings of the First World Conference on Photovoltaic Energy Conversion*, Waikaloa, Hawaii, 1994. IEEE, 1995; 107–110.
6. Rose DH, Hasoon FS, Dhere RG, Albin DS, Ribelin RM, Li X, Mahathongdy Y, Gessert TA, Sheldon P. Fabrication procedures and process sensitivities for CdS/CdTe solar cells. *Progress in Photovoltaics: Research and Application* 1999; **7**: 331–340.
7. Uda H, Matsumoto H, Komatsu Y. All screen printed CdS/CdTe solar cell. In *Proceedings of the 14th Photovoltaic Specialists Conference*, New York, 1982. IEEE, 1983; 801–804.
8. Meyers PV, Liu CH, Doty M. Methods of making photovoltaic cell with chloride dip. US Pat. 4, 873, 198, 1989.
9. Xhou TX, Reiter N, Powell RC, Sasala R, Meyers PV. Vapor chloride treatment of polycrystalline CdTe/Cds films. In *Proceedings of the First World Conference on Photovoltaic Energy Conversion*, Waikaloa, Hawaii, 1994. IEEE, 1995; 103–106.
10. McCandless BE, Hichiri H, Hanket G, Birkmire RW. Vapour phase treatment of CdTe/CdS thin films with $CdCl_2 : O_2$. In *Proceedings of the 25th Photovoltaics Specialists Conference*, Washington, DC, 1996. IEEE, 1997; 781–784.
11. Mahathongdy Y, Albin DS, Wolden CA, Baldwin RM. Vapour $CdCl_2$ optimization and screening experiments for an all dry chloride treatment of CdS/CdTe solar cells. *NCPV Photovoltaics Program Review*, *AIP Conference Proceedings No. 462*, 1999; 236–241.
12. Li X, Ribelin R, Mahathongdy Y, Albin D, Dhere R, Rose D, Asher S, Moutinho H, Sheldon P. The effect of high-resistance SnO_2 on CdS/CdTe device performance. *NCPV Photovoltaics Program Review*, *AIP Conference Proceedings No. 462*, 1999; 230–235.
13. Albin D, Dhere R, Swartzlander-Guest A, Rose D, Li X, Levi D, Niles D, Moutinho H, Matson R, Sheldon P. Interface reactions in CdTe solar cell processing. In *Thin-Film Structures for Photovoltaics: Proceedings of the Materials Research Society Symposium*, 1997, Boston, Massachusetts. Materials Research Society Symposium Proceedings, Vol. 485.
14. Li X, Niles DW, Hasoon FS, Matson RJ, Sheldon P. Effect of nitric-phosphoric acid etches on material properties and back-contact formation of CdTe-based solar cells. *Journal of Vacuum Science and Technology A* 1999; **17**(3): 805–809.
15. Sarlund J, Ritala M, Leskela M, Siponmaa E, Zilliacus R. Characterization of etching procedure in preparation of CdTe solar cells. *Solar Energy Materials and Solar Cells* 1996; **44**: 177–190.
16. Waters DM, Niles D, Gessert TA, Albin D, Rose DH, Sheldon P. Surface analysis of CdTe after various pre-contact treatments. In *Proceedings of the 2nd World Conference on Photovoltaic Solar Energy Conversion*, Vienna, Austria, 1998. WIP, 1999; 1031–1034.
17. Xanio K. *Semiconductors and Semi-metals*, *Vol. 13*, *Cadmium Telluride*, Willardson RK, Beer AC (eds). Academic Press: New York, 1978; 148.
18. Sites JR. Separation of voltage loss mechanisms in polycrystalline solar cells. In *Proceedings of the 20th IEEE Photovoltaic Specialists Conference*, Las Vegas, 1988. IEEE, 1989; 1604–1608.
19. Madelung O, Schultz M, Weiss H. *Semiconductors*, *Group III: Crystal and Solid State Physics*, *Vol. 17*, *Landholt-Bornstein New Series*, *Numerical Data and Functional Relationships in Science and Technology*, Hellwege KH (ed). Springer: Berlin, 1983; 106–117.